Non-Oscillatory Thermal Front Tracking Based on a Reconstructed Discontinuous Galerkin Method for Geothermal Reservoir Simulation

with Its Preliminary Implementation in the MOOSE Framework

Yidong Xia, Hai Huang, and Robert Podgorney
Department of Energy Resource Recovery & Sustainability
Energy and Environment Science & Technology Directorate
Idaho National Laboratory
yidong.xia@inl.gov

Presented at

2015 International Conference on Coupled Thermo-Hydro-Mechanical-Chemical (THMC) Processes in Geosystems

Salt Lake City, Utah, USA

February 25 – 27, 2015

Who Am I?

- Current research focus
  - High-order methods for coupled THMC processes in geosystems
- PhD in Aerospace Engineering with Minor in General Mathematics
- Research interest
  - Computational fluid dynamics and heat transfer
  - High performance computing with GPU

--- Past ---

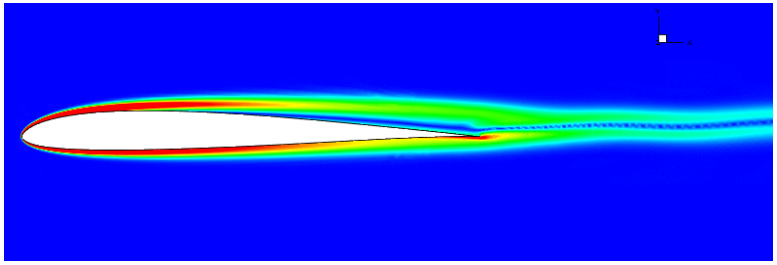

--- Now ---

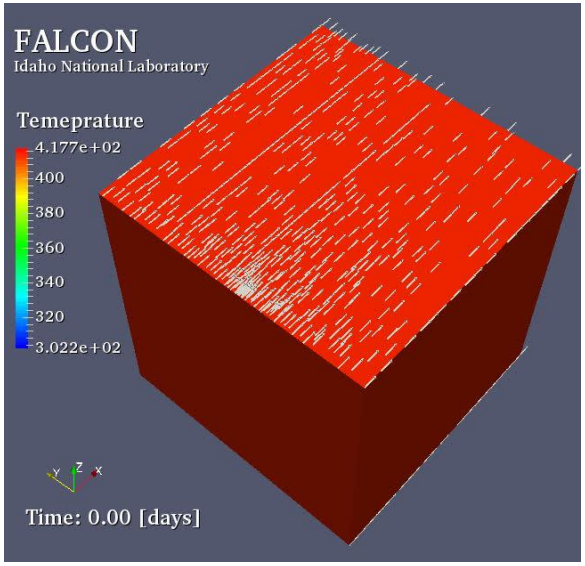

Code Description

- ***FALCON*** code
  - Stands for Fracturing And Liquid CONvection
  - Built based on INL's **MOOSE** framework http://www.mooseframework.com/
  - Physics-based, massively parallel, fully-coupled, **finite element** model for simultaneously solving multiphase fluid Flow, heat transport, and rock deformation for geothermal reservoir simulation

- Collaborative efforts
  - **INL**: Derek Gaston, Cody Permann, Mitch Plummer
  - **U. of Utah**: Luanjing Guo, Jacob Bradford, Raili Taylor, Surya Sunkavalli
  - **Others**: CSIRO, U. of Western Au., U. of NSW, U. of Auckland

MOOSE Project

- MOOSE is an object-oriented FEM framework allowing rapid development of new simulation tools. *Meets NQA-1 requirements*.
- Application development focuses on implementing physics rather than numerical issues.
- Leverages multiple DOE and university developed scientific computational tools
- Used by multiple national labs, universities and industry partners
  - ~25 applications build on the framework

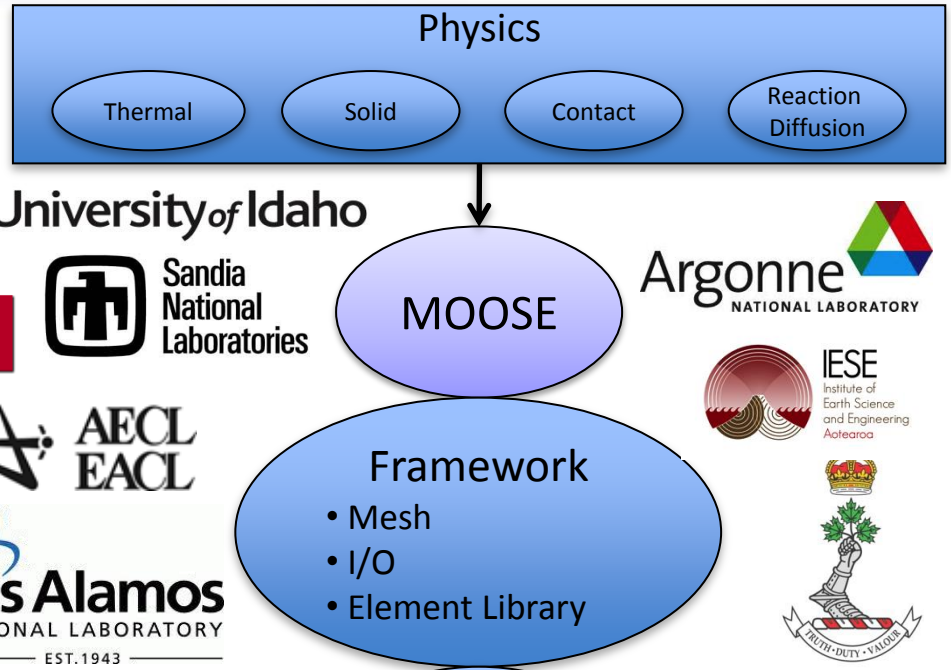

General Capabilities of MOOSE

- 1D, 2D, and 3D
  - User code agnostic of dimension
- Finite Element Based, C++
  - Continuous Galerkin
  - Discontinuous Galerkin
- Fully Coupled/Fully Implicit, “Tight” and “Loose” Coupling Capabilities
- Unstructured Mesh
  - All shapes (Quads, Tris, Hexes, Tets, Pyramids, Wedges…)
  - Higher order geometry (curvilinear, etc.)
  - Reads and writes multiple formats
- Mesh and Timestep Adaptivity
- Parallel
  - User code agnostic of parallelism
- High Order
  - User code agnostic of shape functions

Solution Framework

- MOOSE is based on a Jacobian-Free Newton-Krylov (JFNK) nonlinear solution scheme
- JFNK is ideally suited to solution of large multiphysics systems:
  - Lack of need for Jacobian saves space and time
  - No need to find perfect analytic derivatives (which can be difficult or impossible)
- All physics are solved simultaneously in a fully implicit, fully coupled manner
  - Allows for large time steps
- MOOSE handles all coupling, simultaneously converging all equations
- JFNK uses a Krylov solver and still needs preconditioning

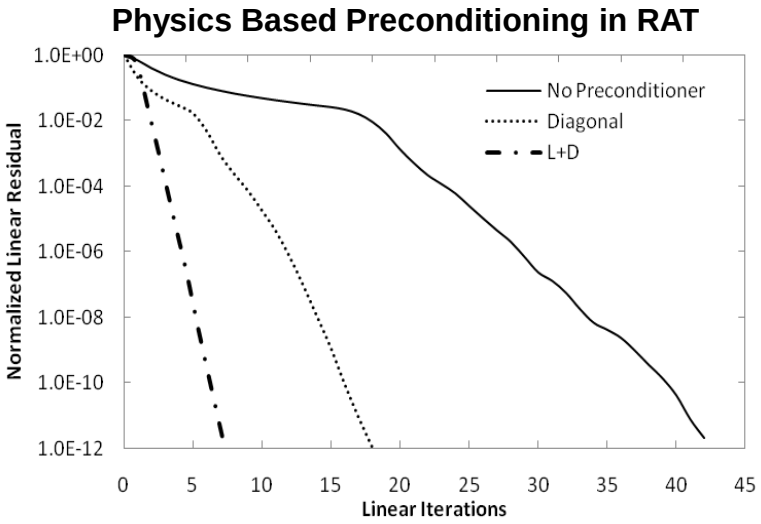

Background

- Main numerical methods for THMC processes in geosystems
  - Finite Difference (FD)
    - ➕ Simple to implement, fast, high-order is feasible
    - ➖ Rigorous requirement in mesh quality; not robust for complex geometries
  - Finite Volume (FV)
    - ➕ Locally conservative; robust and fast; complex geometries
    - ➖ Loss of accuracy in non-conforming mesh and adaptive mesh refinement
  - Finite Element (FE)
    - ➕ High-order accuracy and complex geometries
    - ➕ Suited for multi-physics coupling e.g., fluid-solid
    - ➖ Not well suited for problems with direction, e.g., hyperbolic-type PDEs

No single numerical method can perfectly handle all aspects of THMC!

Background (cont.)

- Example: 1D transport of a steep thermal front with FE
  - A minimal representation of cold fluid injection into a hot fractured zone

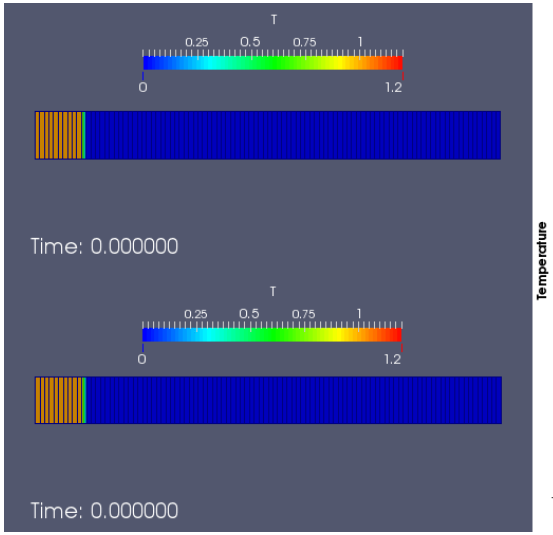

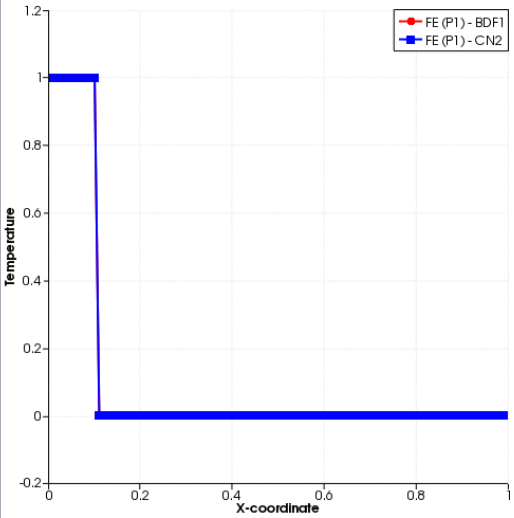

- FE (P1)
  - 2nd-order linear polynomial
- BDF1 – Backward Difference
  - 1st-order time integration
- CN2 – Crank-Nicolson
  - 2nd-order time integration

- Strong non-physical oscillations near thermal front
  - High-order temporal scheme retains oscillations in a wider region
  - Lower-order temporal scheme dissipates the errors, but also decrease accuracy

Background (cont.)

- Exemplary stabilization approaches in the context of FE
  - Streamline Upwind Petrov Galerkin (SUPG), with discontinuity capturing

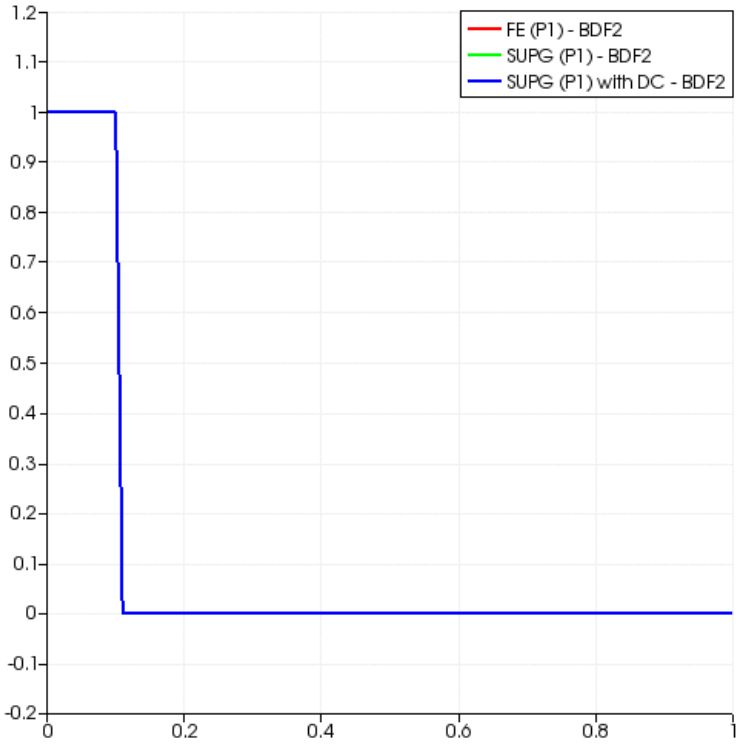

- ❑ Can significantly stabilize transport, but still with over- and under-shoots near the front
- ❑ Formulation strongly depends on the original PDEs, not easy to be modulated
- ❑ Parameters for tuning
- ❑ Alternative FEMs?
  - Flux-Corrected Transport (FCT)-FEM
  - Edge-based FEM
  - Entropy Viscosity Method (EVM)

Motivation

- A non-oscillatory and accurate thermal front tracking technique based on an accurate, robust and flexible numerical method

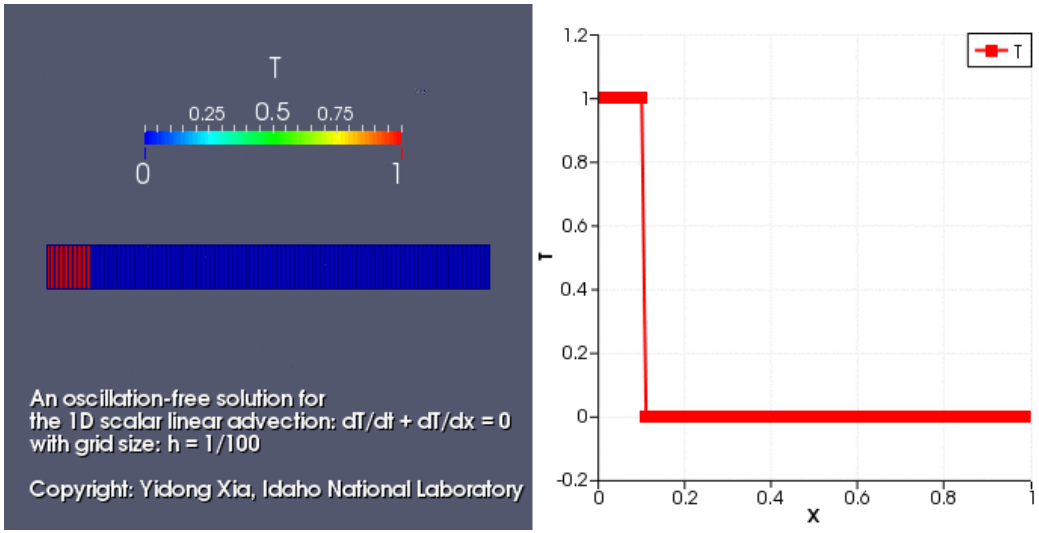

We propose a class of "**reconstructed discontinuous Galerkin**" methods – **rDG**, that combine the advantages of both Finite Element and Finite Volume methods for thermal and hydraulic modeling and simulations in geothermal reservoir

What is Discontinuous Galerkin (DG) Method?

- DG is a variant of the standard (continuous) Galerkin FE method
  - Continuous FE requires continuity of the solution along the element interfaces (edges).
  - DG does NOT require continuity of the solution along edges

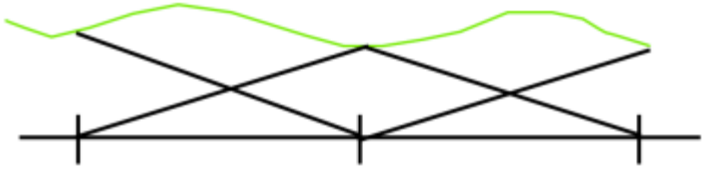

Finite Element

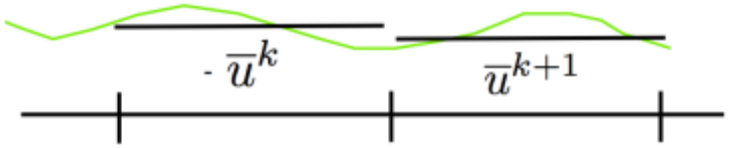

Finite Volume

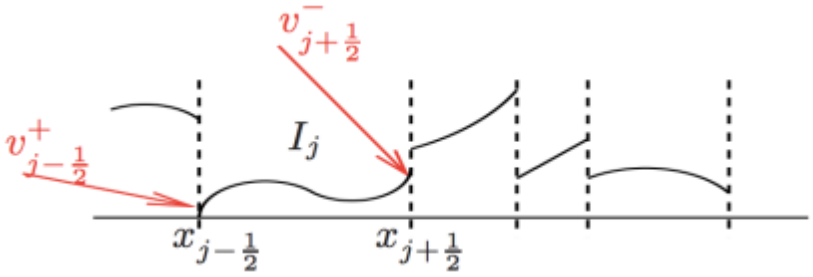

Discontinuous Galerkin

- DG has more degrees of freedom (unknowns) to solve than FE

Features of Discontinuous Galerkin Method

- Why DG?
  - Well suited for complex geometries and non-conforming meshes.
  - Adaptive mesh refinement is easier to implement.
  - Compact and highly parallelizable

- Why not DG?
  - High computational costs (more DOFs for each element)
    - More computing time
    - More storage requirement

Later on I will prove that this is not true!

Choices of Basis Functions: nodal DG

- The DG solution is often represented by the Lagrange basis functions

$$U \approx U_h = \sum_{j=1}^{N} U_j B_j$$

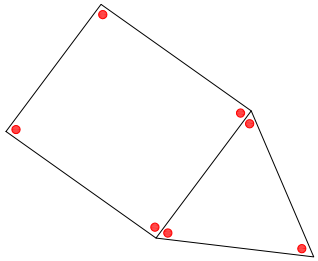

Q1/P1

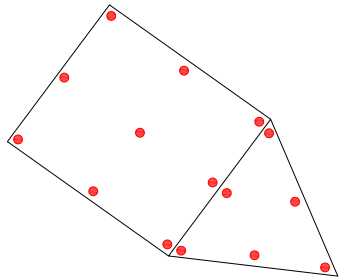

Q2/P2

  - In the case of linear basis, unknowns U_j happen to be on the vertices.
  - Polynomial solutions depend on the shape of elements.

Choices of Basis Functions: modal DG

- Taylor series expansion at the cell centroid, e.g., a P2 polynomial

$$U_h = \bar{U}B_1 + U_x B_2 + U_y B_3 + U_z B_4 + U_{xx} B_5 + U_{yy} B_6 + U_{zz} B_7 + U_{xy} B_8 + U_{xz} B_9 + U_{yz} B_{10}$$

  - The unknowns are cell-averaged variables and their 1st and 2nd derivatives

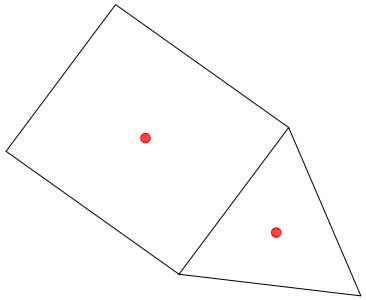

$$B_1 = 1, \quad B_2 = x - x_c, \quad B_3 = y - y_c, \quad B_4 = z - z_c$$

$$B_5 = \frac{B_2^2}{2} - \int_{W_e} \frac{B_2^2}{2}\, dW, \quad B_6 = \frac{B_3^2}{2} - \int_{W_e} \frac{B_3^2}{2}\, dW, \quad B_7 = \frac{B_7^2}{2} - \int_{W_e} \frac{B_7^2}{2}\, dW,$$

$$B_8 = B_2 B_3 - \int_{W_e} B_2 B_3\, dW, \quad B_9 = B_2 B_4 - \int_{W_e} B_2 B_4\, dW, \quad B_{10} = B_3 B_4 - \int_{W_e} B_3 B_4\, dW$$

Features of the Taylor-basis DG

- Same approximate polynomial solution for any shape of elements:
  - Easy to implement on arbitrary shapes of grids
- Handily available cell-averaged variables and their derivatives
  - Easy to implement limiting / discontinuity capturing techniques
- A type of hierarchical basis
  - Easy to implement *p*-multigrid and *p*-adaptivity

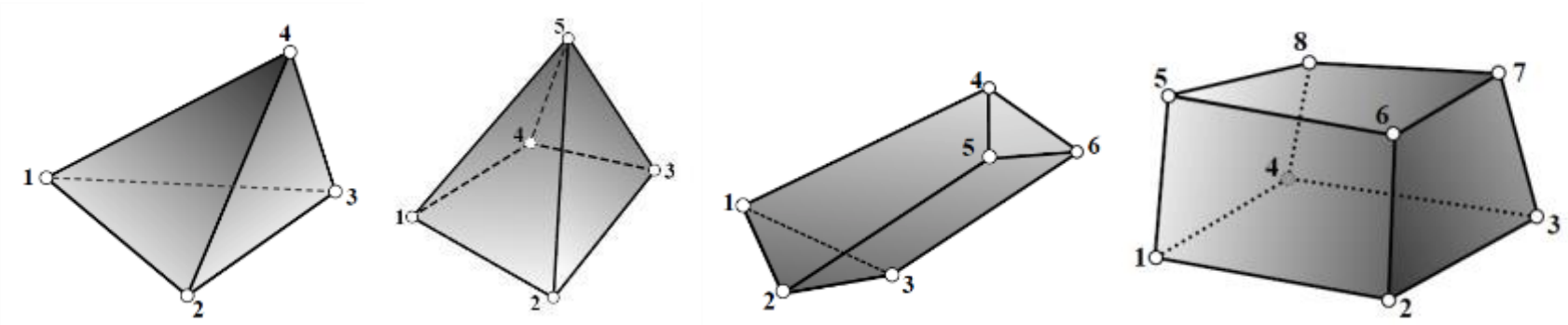

A Generic Convection-Diffusion Equation

- Strong form

$$\frac{\partial U(\mathbf{x}, t)}{\partial t} + \nabla \cdot \left(\mathbf{V} U(\mathbf{x}, t)\right) - \nabla \cdot \nabla \left(D U(\mathbf{x}, t)\right) - F = 0$$

$$\text{with } U_0 = U(\mathbf{x}, 0) \text{ at } t = 0$$

  - U – the variable of interest, e.g., species concentration for mass transfer, temperature for heat transfer
  - $\mathbf{V}$ – the average velocity that the quantity is moving
  - D – the diffusivity
  - F – the “source/sink” term

- A linear case

$$\frac{\partial U(\mathbf{x}, t)}{\partial t} + \mathbf{V} \cdot \nabla U(\mathbf{x}, t) - D \nabla \cdot \nabla U(\mathbf{x}, t) = 0$$

Discontinuous Galerkin Discretization

- Weak form

$$\frac{d}{dt}\int_{\Omega_e} U_h B_i \, d\Omega + \underbrace{\int_{\Gamma_e} (\mathbf{V}U_h)\cdot \mathbf{n} B_i \, d\Gamma}_{\text{Conv. Face Int.}} - \underbrace{\int_{\Omega_e} (\mathbf{V}U_h)\cdot \nabla B_i \, d\Gamma}_{\text{Conv. Domain Int.}} - \underbrace{\int_{\Gamma_e} D\nabla U_h \cdot \mathbf{n} B_i \, d\Gamma}_{\text{Diff. Face Int.}} + \underbrace{\int_{\Omega_e} D\nabla U_h \cdot \nabla B_i \, d\Gamma}_{\text{Diff. Domain Int.}} = 0$$

$$1 \le i \le N$$

  - N – the dimension of the polynomial space
  - B_i – the basis of polynomial function of degree p

- Treatment of non-unique interface fluxes
  - Upwind or solve a Riemann problem like in the case of Finite Volume

Taylor-Basis DG Formulation

- Take another look at the weak form, e.g., DG (P2)

$$\mathrm{W}_e \frac{d\bar{\mathbf{U}}}{dt} + \int_{\mathrm{G}_e} (\mathbf{V} U_h) \cdot \mathbf{n}\, d\mathrm{G} - \int_{\mathrm{G}_e} D \nabla U_h \cdot \mathbf{n}\, d\mathrm{G} = 0, \quad i = 1$$

DG(P0) – nothing but the 1st-order Finite Volume

$$\left[\int_{\mathrm{W}_e} B_j B_i \, d\mathrm{W} \right]_{9\times 9} \frac{d}{dt} \left[U_x,\ U_y,\ U_z,\ U_{xx},\ U_{yy},\ U_{zz}, U_{xy}, U_{xz}, U_{yz} \right]^T + \left[\mathbf{R} \right]_{9\times 1} = 0, \quad 2 \le i, j \le 10$$

  - The cell-averaged variable is decoupled from the derivatives

$$\int_{\mathrm{W}_e} B_1 B_i \, d\mathrm{W} = 0, \quad 2 \le i \le 10$$

  - Finite Volume becomes a subset in Taylor-basis DG formulation!

Hierarchically Reconstructed DG – rDG methods

- A few of the rDG methods in the present study:
  - rDG (P0P1): 2nd-order in space
    - Step 1. Reconstruct the 1st derivatives based on P0 solution
    - Step 2. Limit the 1st derivatives using compact WENO reconstruction at P1
  - rDG (P1P1): 2nd-order in space
    - Step 1. Limit the 1st derivatives using compact WENO reconstruction at P1
  - rDG (P1P2): 3rd-order in space
    - Step 1. Reconstruct the 2nd derivatives based on P1 solution
    - Step 2. Limit the 2nd derivatives using compact WENO reconstruction at P2
    - Step 3. Limit the 1st derivatives using compact WENO reconstruction at P1

------ WENO: Weighted Essentially Non-Oscillatory schemes ------
Refer to the paper for the mathematical description in detail

Numerical Experiments

- Meshes for the first two examples
  - 3D simulation of 1D problems on hexahedral grids
  - Domain bounded by (x, y, z) = ([0, 1], [0, 0.01], [0, 0.01])

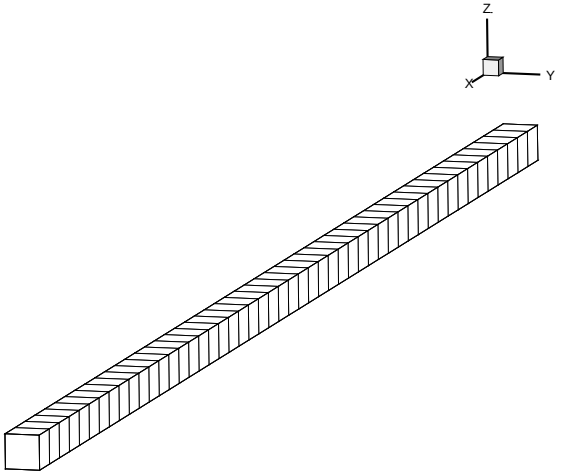

- High-order time integration schemes are applied
- All the examples are conducted in the 3D coordinate system

Example 1. Gaussian Hump in 1D

- A nonlinear wave profile advected by the transport equation:

$$U(x,0) = \exp\left(- b(x - x_0)^2\right) \text{ for } x \hat{I} [0,1]$$

  - The damping coefficient β = 200, and the initial location x_0 = 0.2. All the computations were started at t_0 = 0 and terminated at t = 0.6.

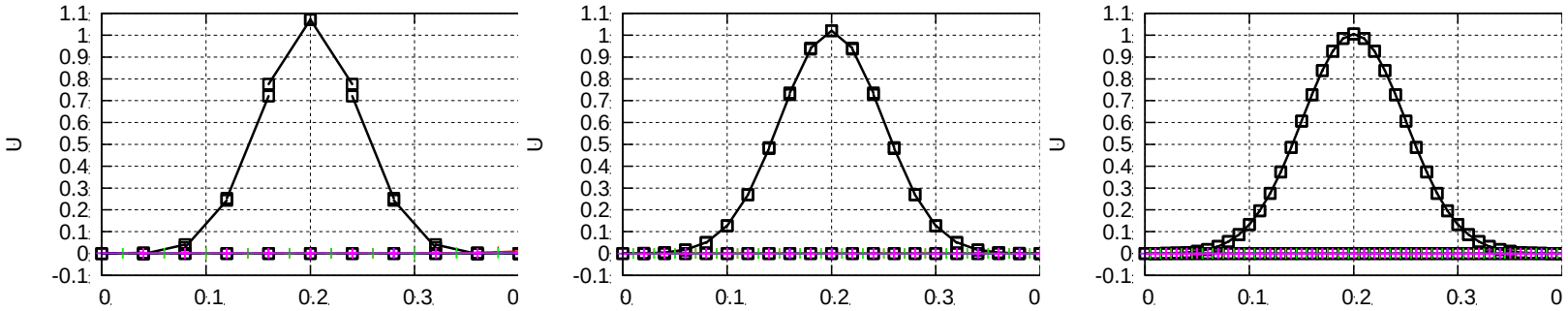

Initial conditions represented by **exact** linear DG solution for h = 1/25, 1/50 and 1/100.

- Objective: error analysis on a smooth convective problem

Example 1. Gaussian Hump in 1D (cont.)

Solution profiles for *h* = 1/25

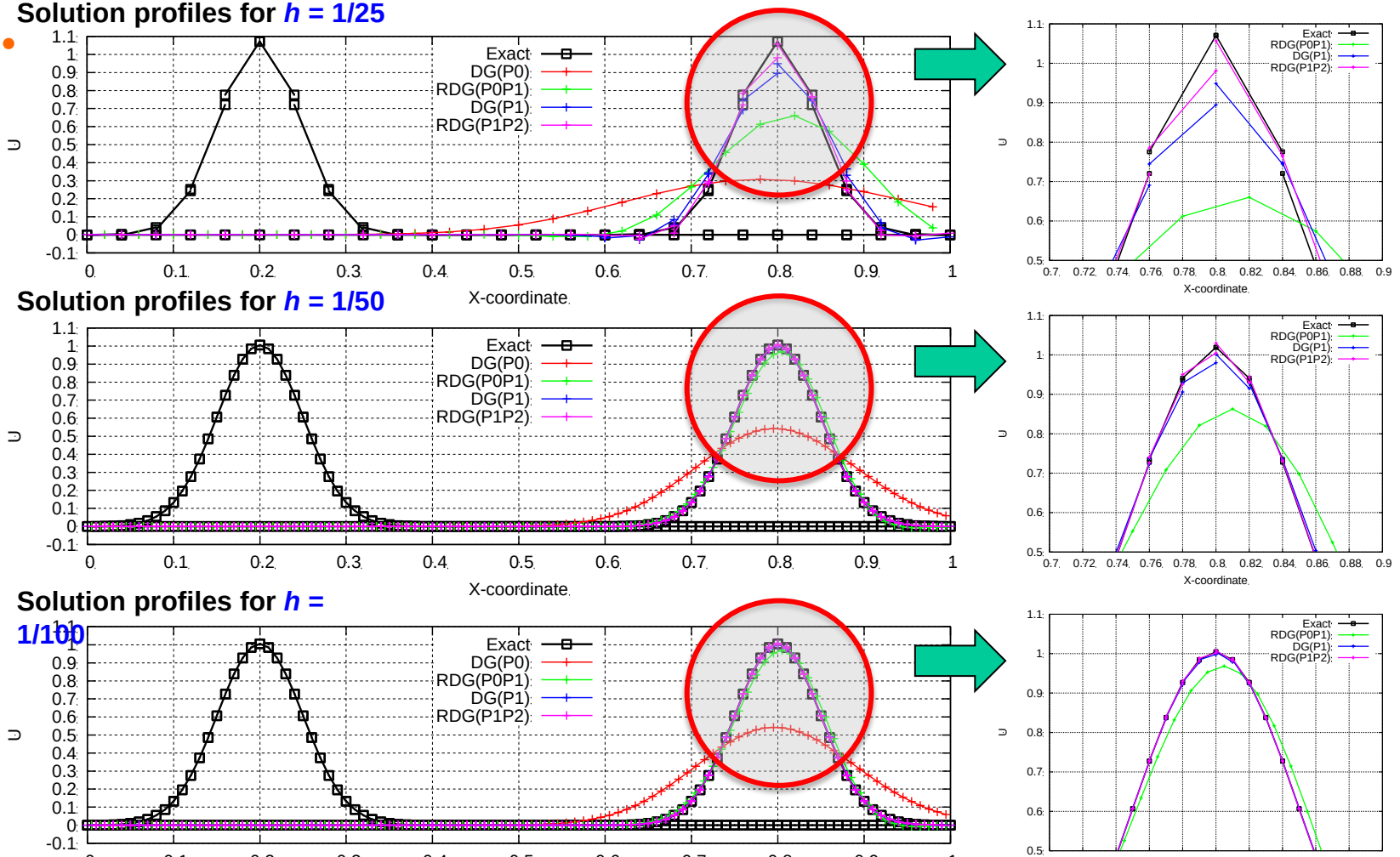

Solution profiles for *h* = 1/50

Solution profiles for *h* = 1/100

Example 1. Gaussian Hump in 1D (cont.)

- Spatial error analysis

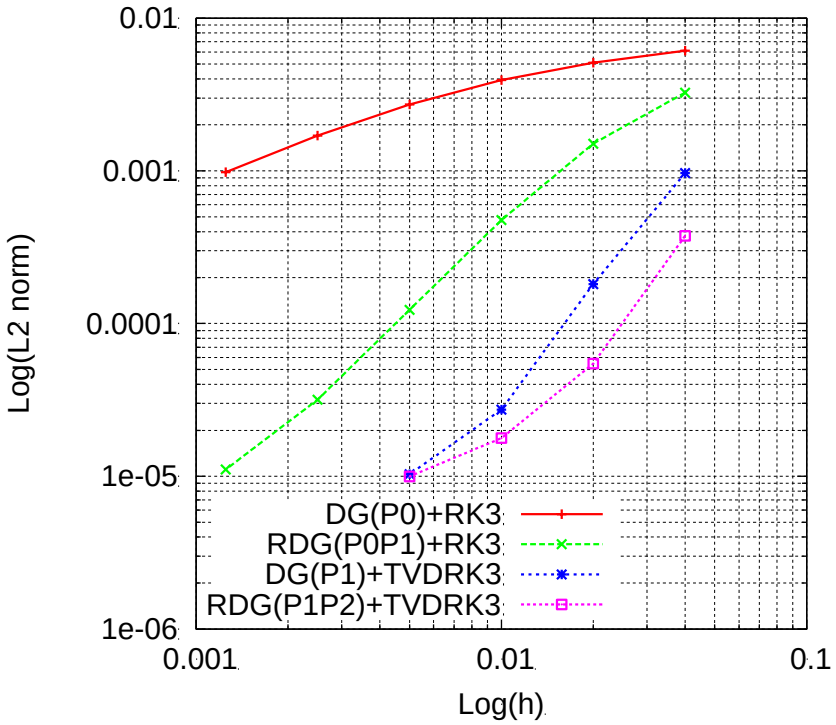

Log(L^2-norm) vs. Log(h)

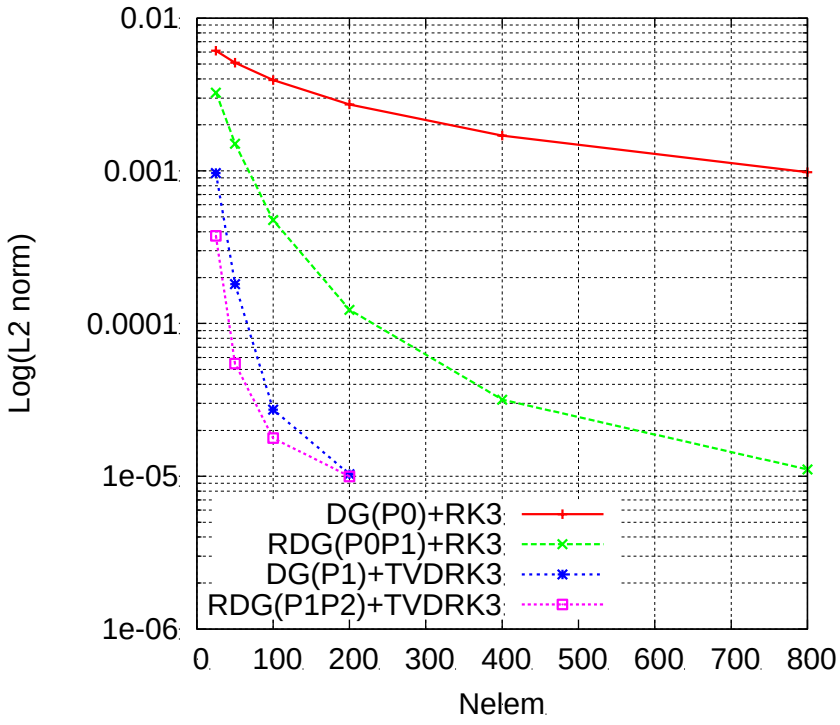

Log(L^2-norm) vs. Nr. of elements

Example 2. Step Function in 1D

- Initial conditions

Left state:	$U = 1.0,\ \mathbf{V} = (1, 0, 0)$	for $x \le 0$
Right state:	$U = 0,\ \mathbf{V} = (1, 0, 0)$	for $0 \le x \le 1$

- Analytical solution to this initial-value-problem

$$U(x,t) = \int_{-\infty}^{0} \frac{1}{\sqrt{4\pi D t}} \exp\left(-\frac{(x - V_x t - \chi)}{4Dt}\right) d\chi$$

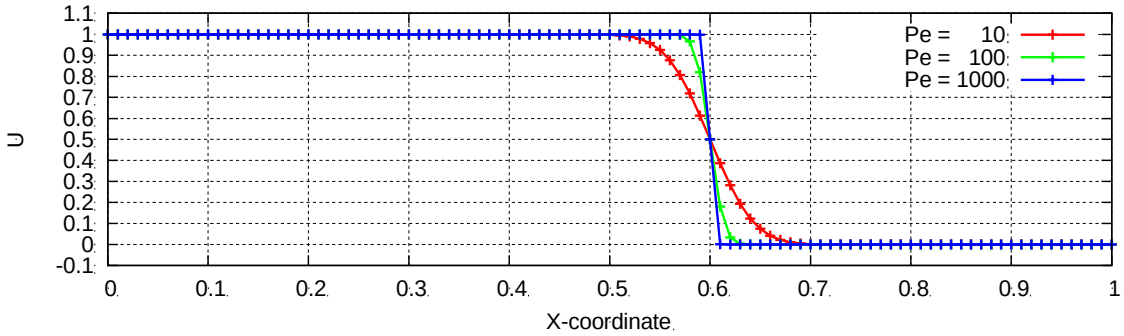

- Useful notations: **DG(P0)** | **rDG(P0P1)** | **DG(P1)** | **rDG(P1P1)** | **rDG(P1P2)**

Solution profiles for *Peclet number = 10*

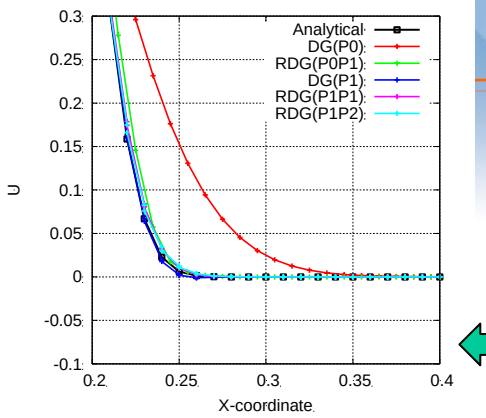

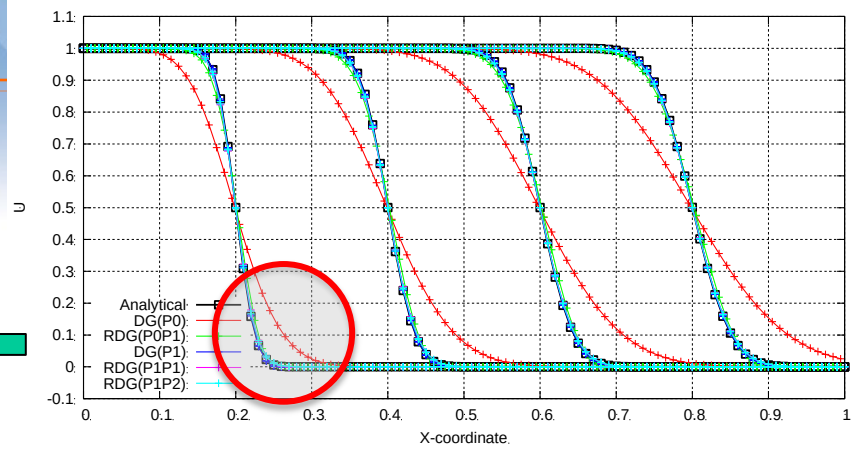

Solution profiles for *Peclet number = 100*

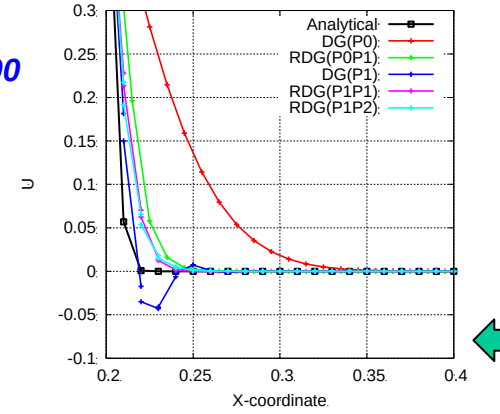

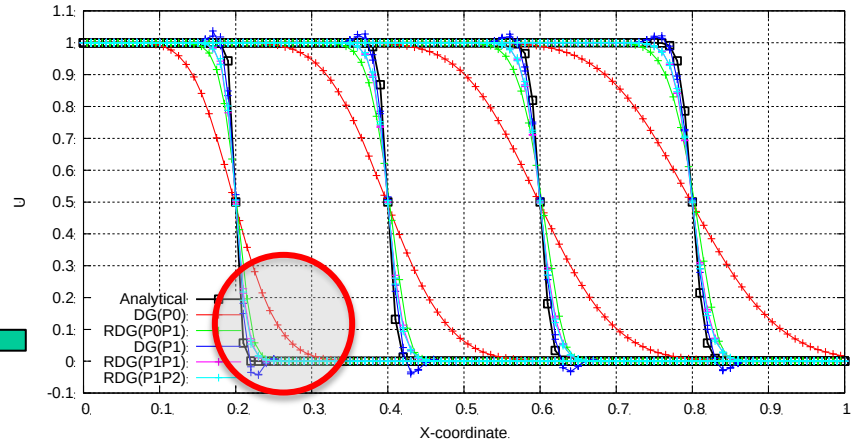

Solution profiles for *Peclet number = 1000*

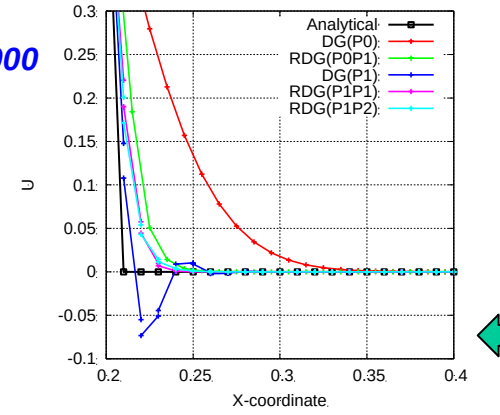

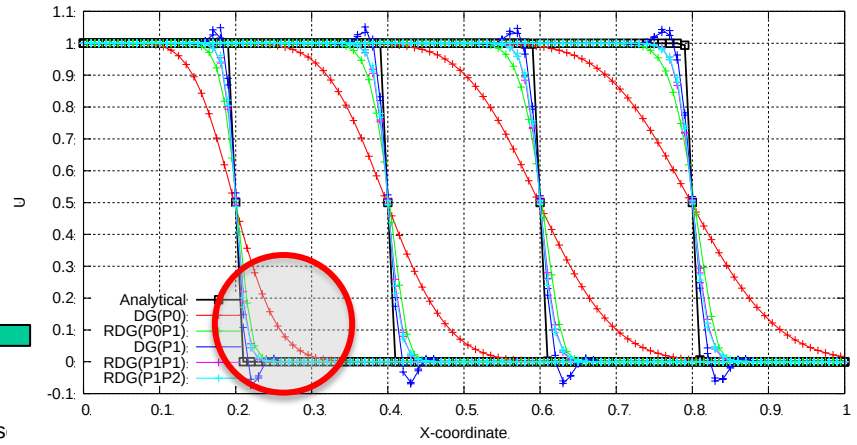

Example 3. Transport of Square Wave in 2D

- Quadrilateral meshes

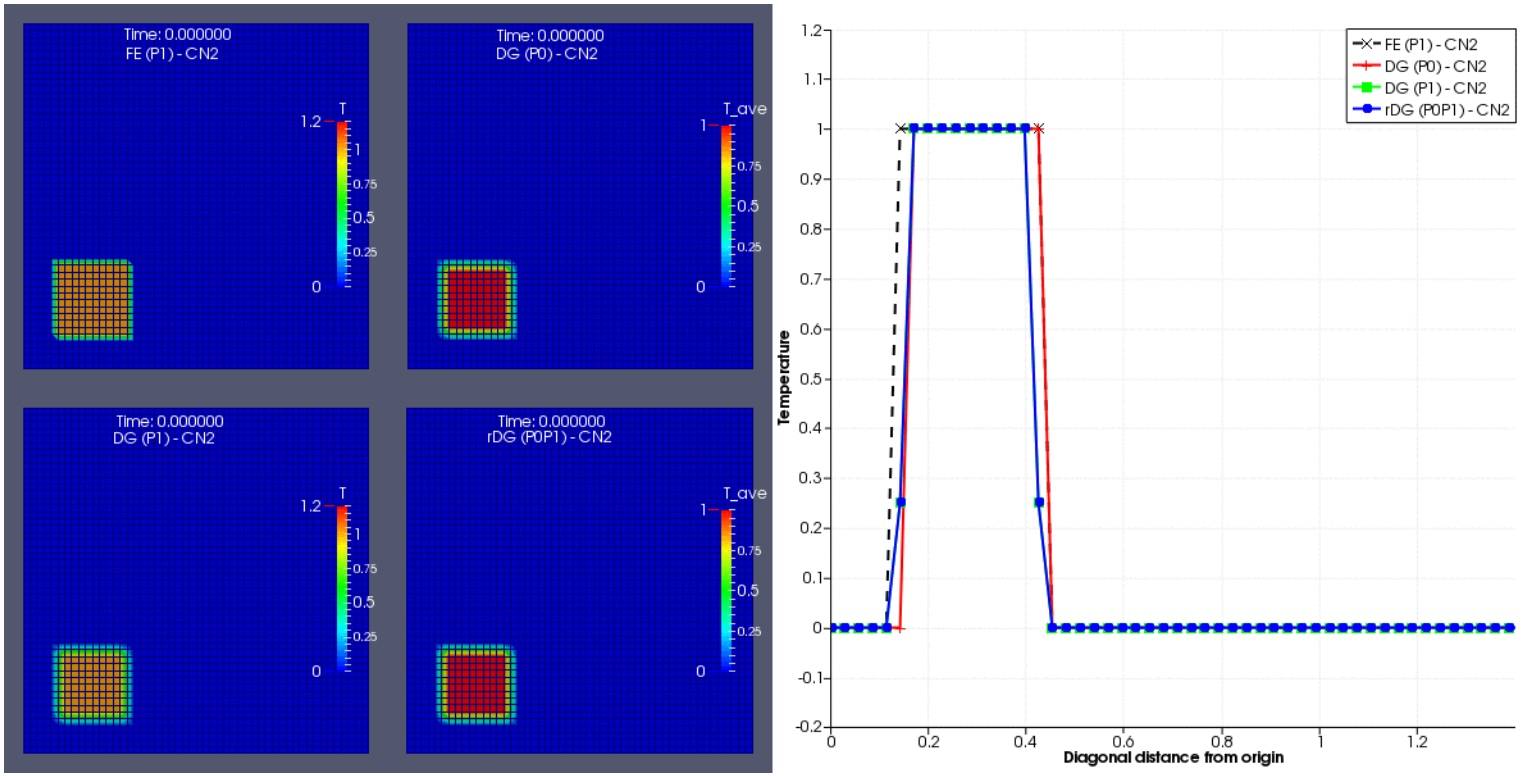

Example 3. Transport of Square Wave in 2D (cont.)

- Triangular meshes

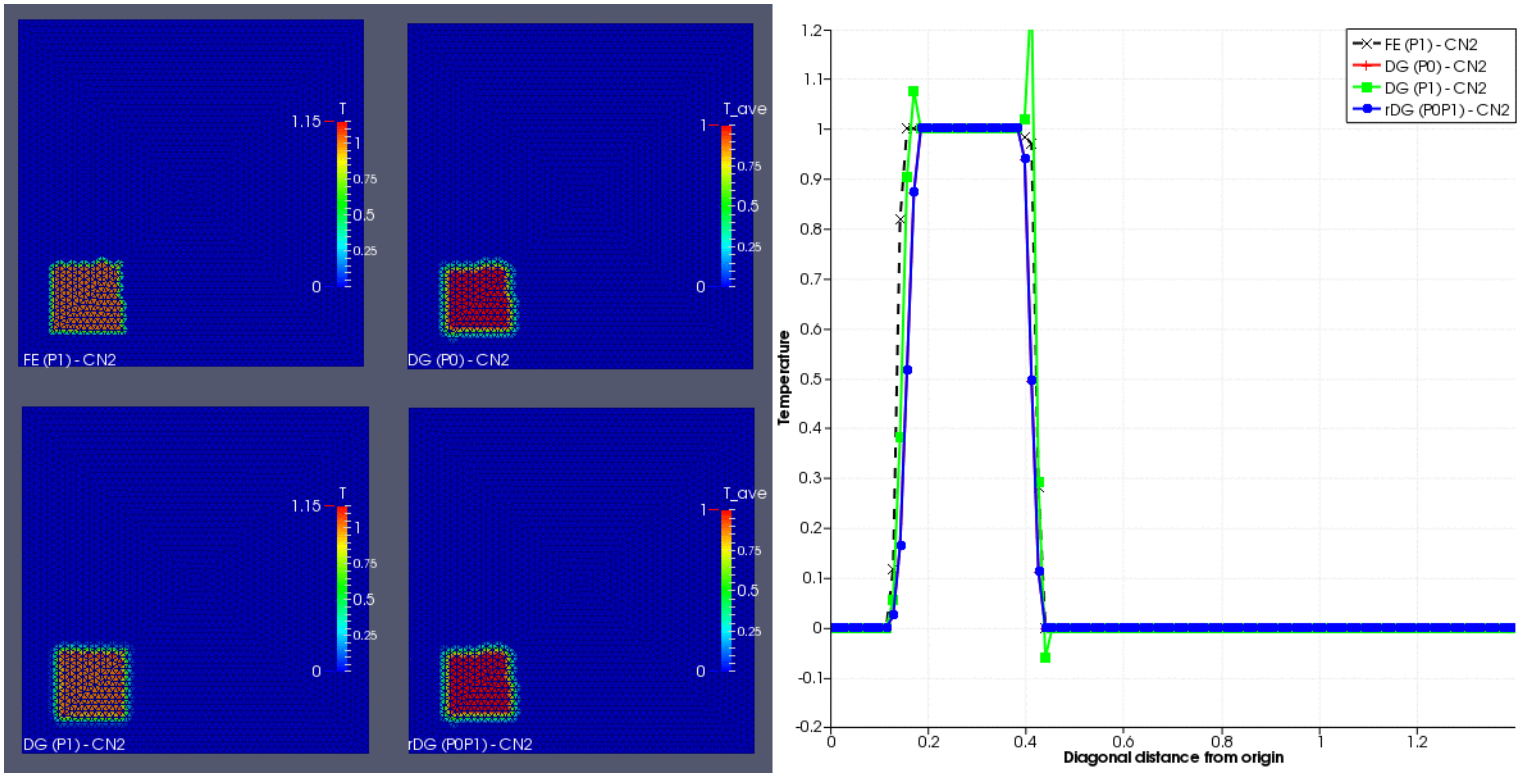

Example 4. Cold Water Injection in 3D

- Injection of cold water through a fractured rock zone
  - Designed Peclet number = 1000 (strongly convective)
  - Domain bounded by (x, y, z) = ([-0.5, 0.5], [-0.5, 0.5], [-0.5, 0.5])
  - Pressure-temperature based thermo-hydro formulation in porous media

$$\begin{cases} \dfrac{\partial r}{\partial t} + \nabla \cdot \left(- r \dfrac{k}{m} \nabla p \right) = 0 \\ \left[f r c_w + (1 - f) r_r c_r \right] \dfrac{\partial T}{\partial t} - \nabla \cdot \left(K_m \nabla p \right) + c_w \mathbf{q} \cdot \nabla T = 0 \end{cases}$$

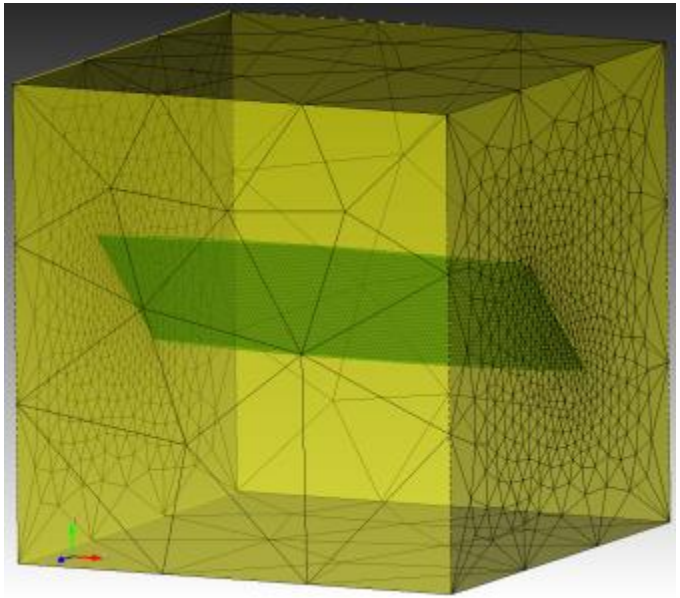

Example 4. Cold Water Injection in 3D (cont.)

- Pressure gradient-induced thermal transport of cold water in a hot fractured rock zone

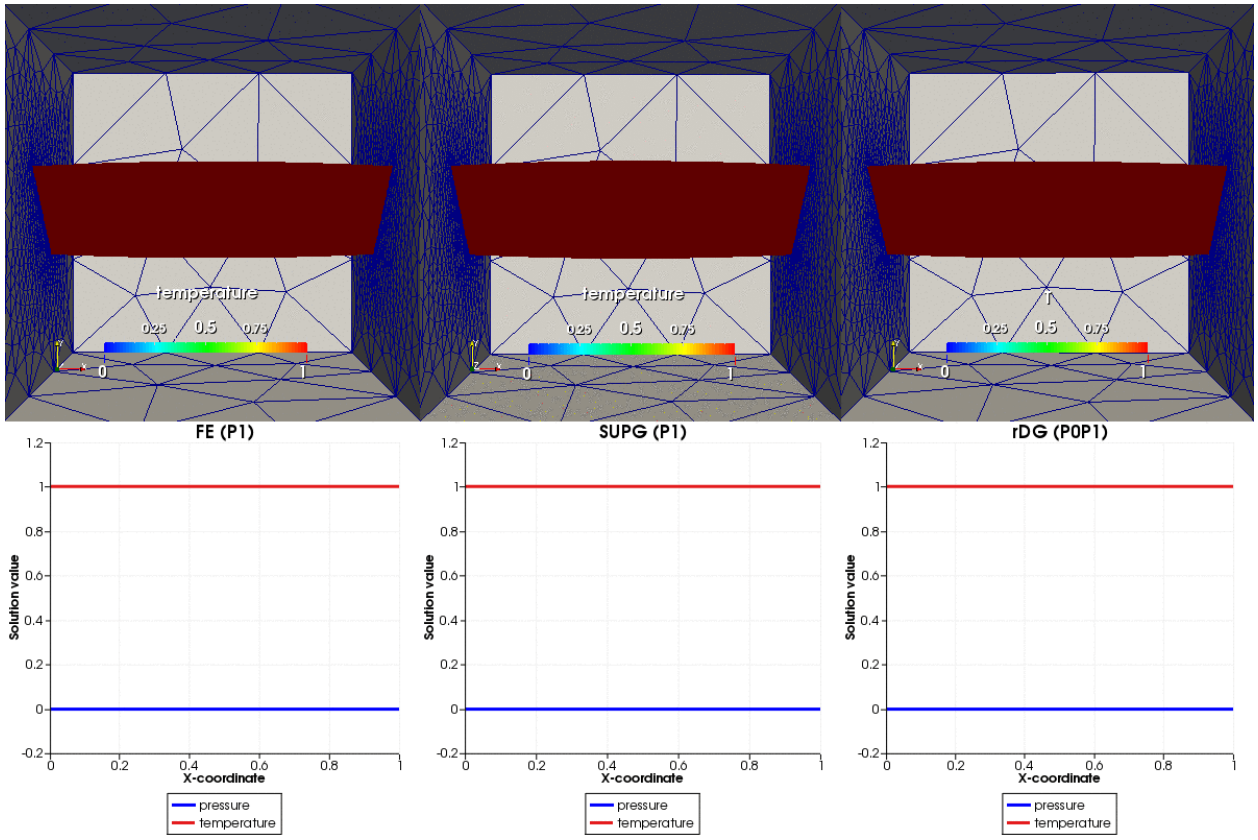

Conclusion

- A class of reconstructed discontinuous Galerkin methods for thermal and hydraulic (TH) modeling and simulation in porous media
  - Effective thermal front tracking without non-physical oscillations
  - Sufficient accuracy
- Limitations
  - Solid mechanics (Finite Element is still the choice here)
- Future work
  - two-phase flow (water and steam)
  - Chemically reactive transport (hyperbolic-type equations)

Acknowledgment

- This work was supported by the U.S. Department of Energy, under a DOE Idaho Operations Office Contract. Accordingly, the U.S. Government retains a nonexclusive, royalty-free license to publish or reproduce the published form of this contribution, or allow others to do so, for U.S. Government purposes.